Robert N. Bone,[1,2] Ying Gai,[2,3] Victoria Magrioti,[4] Maroula G. Kokotou,[4] Tomader Ali,[2,3] Xiaoyong Lei,[2,3] Hubert M. Tse,[2,5] George Kokotos,[4] and Sasanka Ramanadham[2,3]

Inhibition of Ca^{2+}-Independent Phospholipase $A_2\beta$ ($iPLA_2\beta$) Ameliorates Islet Infiltration and Incidence of Diabetes in NOD Mice

Diabetes 2015;64:541–554 | DOI: 10.2337/db14-0097

Autoimmune β-cell death leads to type 1 diabetes, and with findings that Ca^{2+}-independent phospholipase $A_2\beta$ ($iPLA_2\beta$) activation contributes to β-cell death, we assessed the effects of $iPLA_2\beta$ inhibition on diabetes development. Administration of FKGK18, a reversible $iPLA_2\beta$ inhibitor, to NOD female mice significantly reduced diabetes incidence in association with *1*) reduced insulitis, reflected by reductions in $CD4^+$ T cells and B cells; *2*) improved glucose homeostasis; *3*) higher circulating insulin; and *4*) β-cell preservation. Furthermore, FKGK18 inhibited production of tumor necrosis factor-α (TNF-α) from $CD4^+$ T cells and antibodies from B cells, suggesting modulation of immune cell responses by $iPLA_2\beta$-derived products. Consistent with this, *1*) adoptive transfer of diabetes by $CD4^+$ T cells to immunodeficient and diabetes-resistant NOD.*scid* mice was mitigated by FKGK18 pretreatment and *2*) TNF-α production from $CD4^+$ T cells was reduced by inhibitors of cyclooxygenase and 12-lipoxygenase, which metabolize arachidonic acid to generate bioactive inflammatory eicosanoids. However, adoptive transfer of diabetes was not prevented when mice were administered FKGK18-pretreated T cells or when FKGK18 administration was initiated with T-cell transfer. The present observations suggest that $iPLA_2\beta$-derived lipid signals modulate immune cell responses, raising the possibility that early inhibition of $iPLA_2\beta$ may be beneficial in ameliorating autoimmune destruction of β-cells and mitigating type 1 diabetes development.

Type 1 diabetes is a consequence of autoimmune destruction of β-cells, involving activation of cellular immunity leading to infiltration of islets by inflammatory immune cells (1,2). An understudied area is the role lipid signals play in this process. Our studies indicate that the group VIA Ca^{2+}-independent phospholipase $A_2\beta$ ($iPLA_2\beta$) is induced under a diabetic milieu and that mitigation of $iPLA_2\beta$ attenuates β-cell death (3–6). These findings raise the possibility that $iPLA_2\beta$ contributes to β-cell death and consequential diabetes development.

The $iPLA_2\beta$ enzyme is a member of the family of PLA_2s (7) that catalyzes hydrolysis of the *sn*-2 substituent from glycerophospholipid substrates to yield a free fatty acid and a 2-lysophospholipid (8), is widely expressed, and participates in numerous biological processes (9). In the islet, $iPLA_2\beta$ is predominantly localized in β-cells (4,10), which are enriched in arachidonate-containing phospholipid substrates. Following its hydrolysis by $iPLA_2\beta$, arachidonic acid can be metabolized by cyclooxygenase (COX) and lipoxygenase (LOX) to bioactive eicosanoids, many of which are recognized promoters of immune responses (11,12). In view of a described link between $iPLA_2\beta$ and

[1]Department of Pathology, University of Alabama at Birmingham, Birmingham, AL
[2]Comprehensive Diabetes Center, University of Alabama at Birmingham, Birmingham, AL
[3]Department of Cell, Developmental and Integrative Biology, University of Alabama at Birmingham, Birmingham, AL
[4]Laboratory of Organic Chemistry, Department of Chemistry, University of Athens, Athens, Greece
[5]Department of Microbiology, University of Alabama at Birmingham, Birmingham, AL

Corresponding author: Sasanka Ramanadham, sramvem@uab.edu.

Received 17 January 2014 and accepted 2 September 2014.

This article contains Supplementary Data online at http://diabetes.diabetesjournals.org/lookup/suppl/doi:10.2337/db14-0097/-/DC1.

© 2015 by the American Diabetes Association. Readers may use this article as long as the work is properly cited, the use is educational and not for profit, and the work is not altered.

β-cell apoptosis and evidence of its induction in clinical and experimental diabetes (13–15), we considered the possibility that iPLA$_2$β inhibition preserves β-cell mass and mitigates diabetes development.

To date, the *S*-enantiomer of bromoenol lactone (*S*-BEL), with 10 times greater specificity for iPLA$_2$β than iPLA$_2$γ (16), has been used to discern the role of iPLA$_2$β in biological processes. However, several features of BEL, including irreversible inhibition of iPLA$_2$s, nonspecific inhibition of serine-based non-iPLA$_2$ enzymes, and cytotoxicity (9,17), render it less feasible for use as an in vivo inhibitor of iPLA$_2$β.

Fluoroketone (FK) compounds have been synthesized that exhibit selectivity for iPLA$_2$s versus sPLA$_2$s or cPLA$_2$s (18). We demonstrated that FKGK18 is a reversible inhibitor that is 100-fold more specific for iPLA$_2$β than iPLA$_2$γ, does not nonspecifically inhibit other serine proteases, is not cytotoxic, and inhibits β-cell apoptosis (19). These observations suggest that FKGK18 is amenable for in vivo administrations and led us to assess its impact on autoimmune diabetes development. The potential for beneficial effects of inhibiting iPLA$_2$β in vivo with FK compounds is evidenced by amelioration of ovarian cancer and central nervous system–related disorders, in the absence of systemic toxicity, with an earlier generation FKGK inhibitor (20–23).

We report here that FKGK18 administration to spontaneous diabetes–prone NOD mice decreases diabetes incidence, reduces islet infiltration, improves glucose homeostasis, and preserves β-cell area. Furthermore, FKGK18 inhibits immune cell function and adoptive transfer of diabetes. These findings suggest that iPLA$_2$β activation promotes immune responses and that iPLA$_2$β inhibition may be beneficial in ameliorating diabetes.

RESEARCH DESIGN AND METHODS

iPLA$_2$β Message

Islet RNA was prepared from 6–7-week-old female C57BL/6J, NOD, NOD.*scid*, and NOD.*Rag* mice and male NOD mice (The Jackson Laboratory, Bar Harbor, ME), and cDNA was prepared for quantitative RT-PCR (RT-qPCR) analyses as previously described (3). Primers were based on mouse sequences for iPLA$_2$β and internal control 18S (gene IDs 53357 and 19791, respectively).

Animal Treatment and Monitoring

Female NOD mice were generated and maintained according to University of Alabama at Birmingham Institutional Animal Care and Use Committee policies. Mice were administered intraperitoneally three times per week vehicle (PBS + 5% Tween 80) or FKGK18 [20 mg/kg body weight (20)] from 10 days until euthanized. Body weights and blood glucose levels, measured from tail vein blood samples (2 μL) with the Breeze 2 Blood Glucose Monitoring System (Bayer Healthcare, Mishawaka, IN), were recorded weekly. Diabetes incidence was based on two consecutive blood glucose readings ≥15.3 mmol/L, at which time the mouse was euthanized. By 30 weeks, all mice were euthanized, and blood was collected in BD Microtainer Tubes with serum separator for insulin measurements (ELISA Kit; Mercodia, Uppsala, Sweden).

Tissue Analyses

Paraffin sections (10 μm) of pancreas, heart, liver, and kidney were stained with hematoxylin-eosin (H-E) for histological assessment. Islet images were captured, and total islet and noninfiltrated areas (pixels) were determined.

FKGK18 Bioavailability

Submandibular vein blood from mice was obtained between 0 and 72 h following FKGK18 administration. To 100 μL of serum sample, 1 mL of chloroform and 50 μL of 1 mol/L aqueous hydrochloric acid were added and the mixture vortexed for 30 s, centrifuged for 5 min, and the organic layer transferred to a clean tube. The remaining aqueous layer was re-extracted with 1 mL of chloroform by the same procedure. The two organic layers were combined, dried, reconstituted in methanol, and analyzed for FKGK18 by high-resolution mass spectrometry, recorded with a quadrupole time-of-flight Bruker maXis impact instrument using negative ion mode electrospray ionization protocol. Data acquisition was carried out with Bruker Daltonics DataAnalysis 4.1.

Urine Prostaglandin E$_2$ Metabolite Analyses

Prostaglandin E$_2$ (PGE$_2$) metabolite levels in urine, collected from individual mice housed in metabolic cages over an 18-h period in the absence of food but free access to water, were determined by enzyme immunosorbent assay (Cayman Chemical, Ann Arbor, MI) and normalized to urine creatinine levels measured by colorimetric assay (Cell Biolabs, Inc., San Diego, CA).

Glucose Tolerance

At 25 weeks of age, overnight-fasted mice were administered glucose 2 g/kg body weight in filter-sterilized dH$_2$O i.p., and tail vein blood samples (2 μL) were collected over a 2-h period for glucose measurement. The mice had free access to water during this time.

Immunofluorescence Analyses and β-Cell Area

Paraffin sections (10 μm) of pancreata were processed for immunostaining using an antigen retrieval protocol as previously described (24,25). Sections were incubated overnight at 4°C with 1° antibodies guinea pig anti-insulin (1:200) (Life Technologies, Carlsbad, CA), rat anti-CD4 (1:50) (Santa Cruz Biotechnology, Santa Cruz, CA), rat anti-CD8α (1:50) (Santa Cruz), or rabbit anti-B220 (1:100) (BD Biosciences, San Jose, CA) and subsequently with fluorescence-labeled 2° antibodies Texas Red and fluorescein isothiocyanate–conjugated antibodies (1:200) (Santa Cruz and Jackson ImmunoResearch, West Grove, PA) in the dark (2 h, room temperature). Nuclei were stained with Hoechst 2 μg/mL for 10 min, and the ratio of total insulin-stained islet region to H-E–stained pancreas section was used to calculate β-cell area.

T-Cell and B-Cell Stimulation Assays

Single-cell splenocyte suspensions were prepared from 8–12-week-old NOD mice. $CD4^+$ T cells were purified using the BD IMag CD4 T Lymphocyte Enrichment Set - DM (BD Biosciences), and resting B cells were purified using BD IMag B Lymphocyte Enrichment Set - DM (BD Biosciences), per manufacturer's instructions. $CD4^+$ T cells (2.5×10^5/well) were seeded in 96-well plates coated with αCD3 (1 μg/mL) (BioLegend, San Diego, CA) with media containing αCD28 (0.5 μg/mL) (BioLegend). Cytokine concentrations (48 and 72 h) in the supernatant were measured by ELISA (interleukin [IL]-2 and interferon-γ [IFN-γ] [BD Biosciences] and TNF-α [R&D Systems, Minneapolis, MN]) as previously described (26). B cells (2.5×10^5/well) were seeded in 96-well plates for 72 h with media containing 1 μg/mL lipopolysaccharide (LPS) (Life Technologies) and 2 ng/mL IL-4 (R&D Systems) as previously described (27). IgG and IgM antibody production were measured in the supernatant from the B cells by ELISA (SouthernBiotech, Birmingham, AL) as previously described (28).

MTT Viability Assay

Immune cells were incubated for 3.5 h at 37°C in wells with 3-(4,5-dimethyl-2-thiazolyl)-2,5-diphenyl-2H-tetrazolium bromide (MTT) (Sigma-Aldrich, 20 μL of 5 mg/mL solution). Media were carefully aspirated and replaced with an equal volume of MTT solvent (4 mmol/L HCl and 0.1% Nonidet P-40 in isopropanol). The plate was agitated on a shaker in the dark for 15 min, and absorbance was read at 590 nm.

Adoptive Transfer

Single-cell splenocyte suspensions were prepared from 12-week-old male BDC2.5/NOD mice, as previously described (29). $CD4^+$ T cells were purified, activated in six-well plates (5×10^6 cells/well) coated with αCD3 and αCD28 (1 μg/mL each), and expanded with media containing 100 U/mL IL-2 for 72 h. They were further expanded into T-75 flasks (5×10^6 cells/flask) with media containing 100 U/mL IL-2 for 72 h, collected, washed twice with Hanks' balanced salt solution (HBSS), and diluted to 5×10^6 cells/mL in HBSS. Recipient 6-week-old immunodeficient male NOD.*scid* mice were divided into control and T cells ± FKGK18–administered groups, and diabetes incidence was monitored for 14 days.

Microscopy

Pancreas section and islet images were captured on an Olympus IX81 microscope using cellSens Dimension software and analyzed using ImageJ software (National Institutes of Health).

Statistical Analyses

Data were converted to mean ± SEM and Student *t* test was applied to determine significant differences between two groups ($P < 0.05$). Incidence of diabetes was plotted as a survival curve and analyzed by Mantel-Cox test.

RESULTS

$iPLA_2\beta$ Expression in NOD Mice

RT-qPCR analyses revealed three- to fivefold higher $iPLA_2\beta$ mRNA in islets from 6- to 7-week-old spontaneous diabetes-prone female NOD mice relative to age-matched diabetes-resistant female C57BL/6J, NOD.*scid*, and NOD.*Rag* and male NOD mice (Fig. 1*A*). Because NOD mice exhibit insulitis by 4–6 weeks of age and develop spontaneous diabetes by 10–20 weeks of age (30), these findings raise the possibility that an early increase in $iPLA_2\beta$ contributes to diabetes development.

FKGK18 Bioavailability and In Vivo $iPLA_2\beta$ Inhibition

Female NOD mice were administered vehicle or FKGK18 starting at 10 days of age (Fig. 1*B*), and FKGK18 bioavailability was determined by high-resolution mass spectrometry. Standard FKGK18 (molecular weight 280 g/mol) generated a predominant parent $[M\text{-}H]^-$ ion at charge/mass ratio (m/z) 279 (Fig. 1*C*) and electrospray ionization tandem mass spectrometry (ESI/MS/MS) analyses revealed signature ions at m/z 209.0970, arising from the loss of CHF_3 $[M\text{-}H\text{-}CHF_3]^-$, and m/z 68.9945, representing $[CHF_3\text{-}H]^-$, from the parent ion (Fig. 1*D*). Analyses of NOD serum from mice treated with FKGK18 for >15 weeks generated a similar spectrum profile (Fig. 1*E*) and revealed maximum levels of FKGK18 between 2 and 6 h (~300 ng/mL), which decreased to 70–280 ng/mL by 20–24 h, 0–30 ng/mL by 44–48 h, and were undetectable by 72 h after the last injection. Because the reversible nature of FKGK18 precludes in vivo $iPLA_2\beta$ activity measurement, urinary 13,14-dihydro-15-keto metabolite of PGE_2 (PGEM) levels were measured and found to be decreased up to 42 h but returned to vehicle levels between 48 and 66 h (Fig. 1*F*). Taken together, it was deduced that the in vivo inhibitory effects of FKGK18 20 mg/kg i.p. persist for nearly 48 h.

FKGK18 Reduces Diabetes Incidence and Improves Glucose Homeostasis Without Causing Systemic Toxicity

The FKGK18 regimen did not affect body weight (Fig. 2*A*) or promote discernible tissue damage (Fig. 2*B*) compared with vehicle. However, diabetes incidence was significantly reduced with FKGK18 (Fig. 2*C*). Consistent with literature reports of an ~80% incidence in female NOD mice (30), seven of nine (78%) vehicle-treated mice became diabetic by 25 weeks. In contrast, only 1 of 11 FKGK18-treated mice became diabetic by 25 weeks. At this age, five mice in each group were euthanized for further analyses. Among the remaining six in the FKGK18 group, one additional mouse became diabetic at 28 weeks. The lower diabetes incidence in the FKGK18 group was associated with twofold higher circulating insulin compared with the vehicle group (Fig. 2*D*). Intraperitoneal glucose tolerance testing revealed that although basal overnight-fasted blood glucose levels were similar in the vehicle and FKGK18 groups, they remained lower in the FKGK18 group over the test period (Fig. 2*E*). This was reflected by a 31% reduction in the area under curve

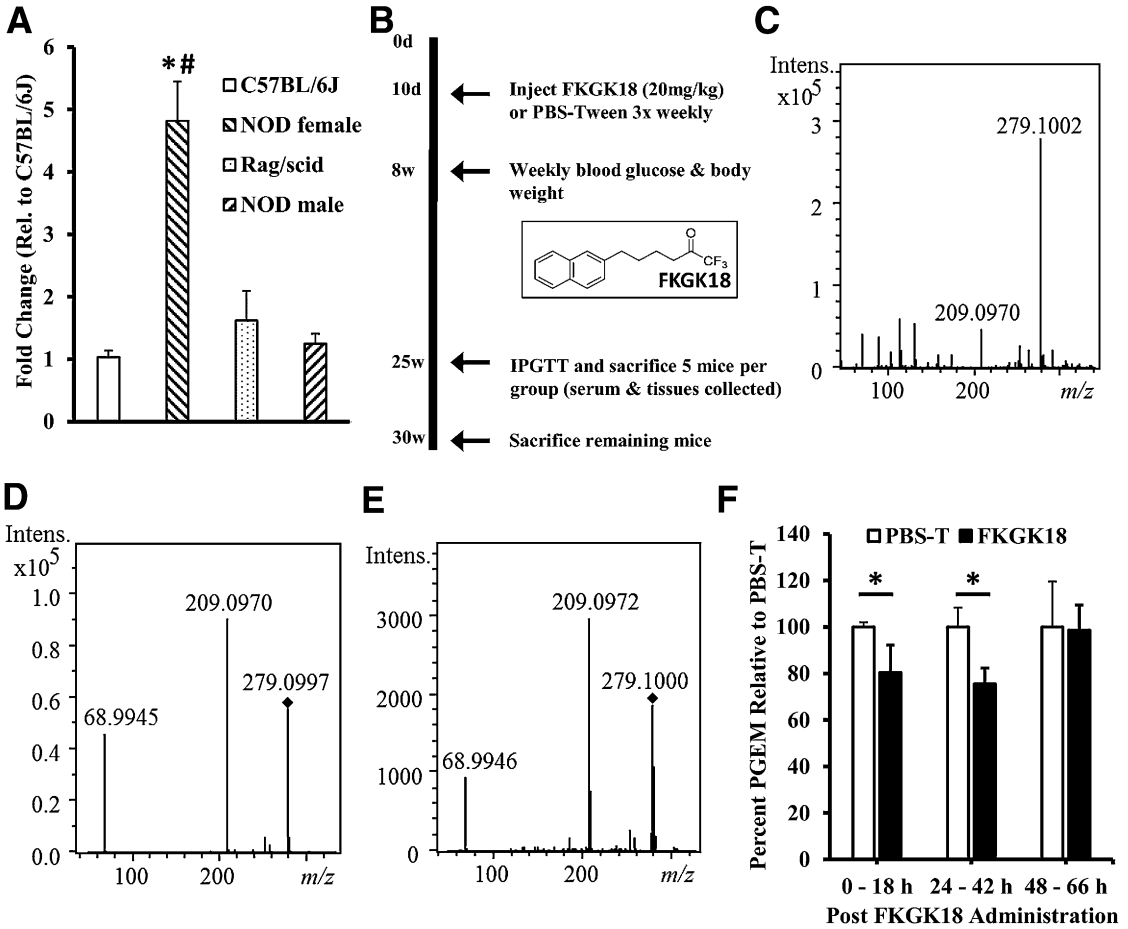

Figure 1—iPLA$_2$β expression, FKGK18 administration, and in vivo evidence for iPLA$_2$β inhibition in NOD mice. *A*: RT-qPCR analyses of iPLA$_2$β was performed using cDNA generated from total RNA prepared from islets isolated from female C57BL/6J, NOD, NOD.*scid*, and NOD.*Rag* mice and male NOD mice (6–7 weeks of age). Fold changes relative to NOD.*scid* are presented as mean ± SEM. *$P < 0.05$ vs. NOD.*scid*/NOD.*Rag*; #$P < 0.0001$ vs. C57BL/6J and NOD male ($n = 3$ pools of 5–8 mice each). *B*: Experimental protocol. *C* and *D*: High-resolution mass spectrometry analyses of FKGK18 standard (0.50 μg/mL). Total ion spectrum showing the parent ion at m/z 279.1002 (*C*) and ESI/MS/MS spectrum showing signature daughter ions at m/z 209.0970 and 68.9945 (*D*). *E*: ESI/MS/MS spectrum of FKGK18 in serum from NOD mice 6 h postadministration (20 mg/kg i.p.). *F*: PGEM assay. Mice under treatment for 10 weeks were housed individually in metabolic cages, and urine was collected overnight (18 h), starting immediately (0–18 h), 24 h (24–42 h), and 48 h (48–66 h) after last administration of vehicle or FKGK18. PGEM measured by enzyme immunosorbent assay and normalized to urine creatinine is presented as mean ± SEM of PGEM relative to vehicle treatment. *$P < 0.05$ vs. corresponding vehicle group ($n = 6$ per group). Intens., intensity; IPGTT, intraperitoneal glucose tolerance test; PBS-T, PBS + 5% Tween 80; Rel., relative.

of the FKGK18 group (Fig. 2*F*), indicating better glucose homeostasis relative to the vehicle group.

FKGK18 Reduces Insulitis and Preserves β-Cell Area

As expected, significant infiltration was evident in islets from the vehicle group (Fig. 3*A*, left panels). In contrast, insulitis was markedly reduced in the FKGK18 group and when present, was predominantly in the peri-islet region (Fig. 3*A*, right panels). Percent islet infiltration, determined by measuring total islet and noninfiltrated areas, revealed 54% infiltration of islets in the vehicle group (128 from 9 mice) but only 35% infiltration of islets in the FKGK18 group (195 from 11 mice) (Fig. 3*B*). Breakdown of the infiltration spectrum (none to complete [0–100%]) revealed twice as many infiltrate-free islets and one-half as many islets with 75–100% infiltration in the FKGK18 group compared with the vehicle group (Fig. 3*C*). Consistent with the improved islet integrity, insulin staining area (Fig. 3*D*) relative to total pancreas section area was sevenfold greater (Fig. 3*E*) in the FKGK18 group, suggesting greater preservation of residual β-cell mass relative to the vehicle group.

FKGK18 Effects on Infiltration by Immune Cell Populations

In view of reduced islet infiltration in the FKGK18 group, immunofluorescence analyses were used to estimate abundance in the infiltrate of CD4$^+$ and CD8$^+$ T cells and B cells, key components of autoimmune diabetes development (2). As shown in Fig. 4*A*, evidence of CD4$^+$ T cells (*i* and *ii*, *iii* and *iv*), CD8α$^+$ T cells (*v* and *vi*, *vii* and *viii*), and B cells (*ix* and *x*, *xi* and *xii*) was found in

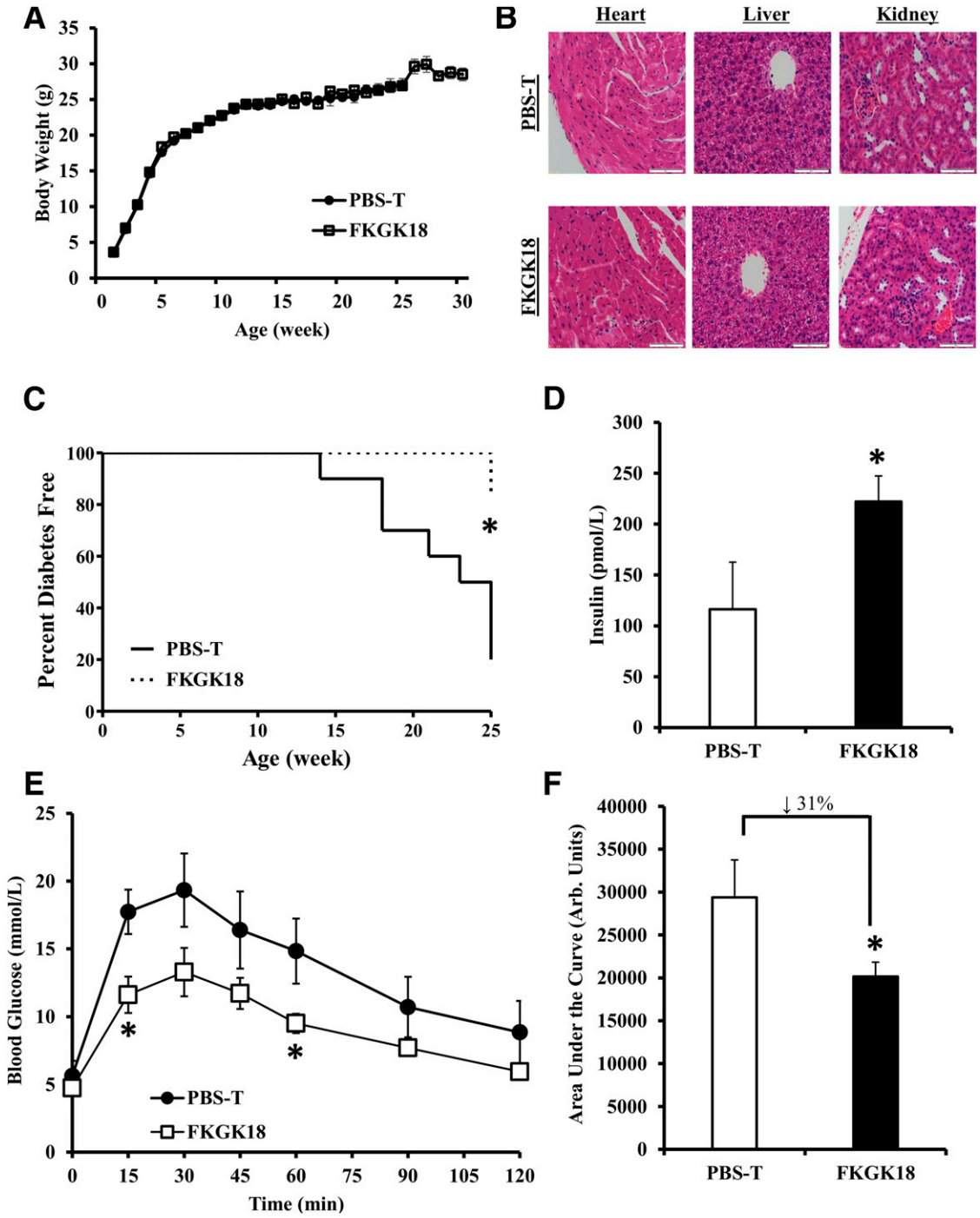

Figure 2—Body weight, tissue histology, diabetes incidence, and glucose tolerance testing. Female NOD mice were injected intraperitoneally with vehicle (PBS + 5% Tween 80 [PBS-T]) or FKGK18 (20 mg/kg, three times per week) from 10 days until euthanasia. *A*: Body weights. Weekly recordings in vehicle (n = 9) and FKGK18 (n = 11) groups. *B*: Tissue histology. At euthanasia, heart, liver, and kidney were excised and processed for H-E staining. Representative images (three random fields captured per mouse) are shown. Original magnification ×400, scale bar = 50 μm. *C*: Diabetes incidence. Blood glucose was monitored weekly, and onset of diabetes was recorded in vehicle-treated and FKGK18-treated mice when two consecutive readings ≥15.3 mmol/L were obtained. *P = 0.015, FKGK18 group vs. vehicle group, Mantel-Cox test (n = 9–11 per group). *D*: Serum insulin. At euthanasia, blood was collected, and serum levels of insulin were determined by ELISA. Data are mean ± SEM. *P < 0.05, FKGK18 group vs. vehicle group (n = 7–10). *E*: Intraperitoneal glucose tolerance testing (IPGTT). Mice treated with vehicle or FKGK18 for 25 weeks were fasted overnight before obtaining basal blood glucose levels. The mice were then administered glucose 2 g/kg body weight, and blood glucose in a 2-μL aliquot of tail vein blood was monitored over a 2-h period. *P < 0.05, FKGK18 group vs. vehicle group. *F*: Area under the curve. Data obtained through the IPGTT were used to calculate the area under the curve, an index of glucose tolerance. *P < 0.05, FKGK18 group vs. vehicle group. Arb., arbitrary.

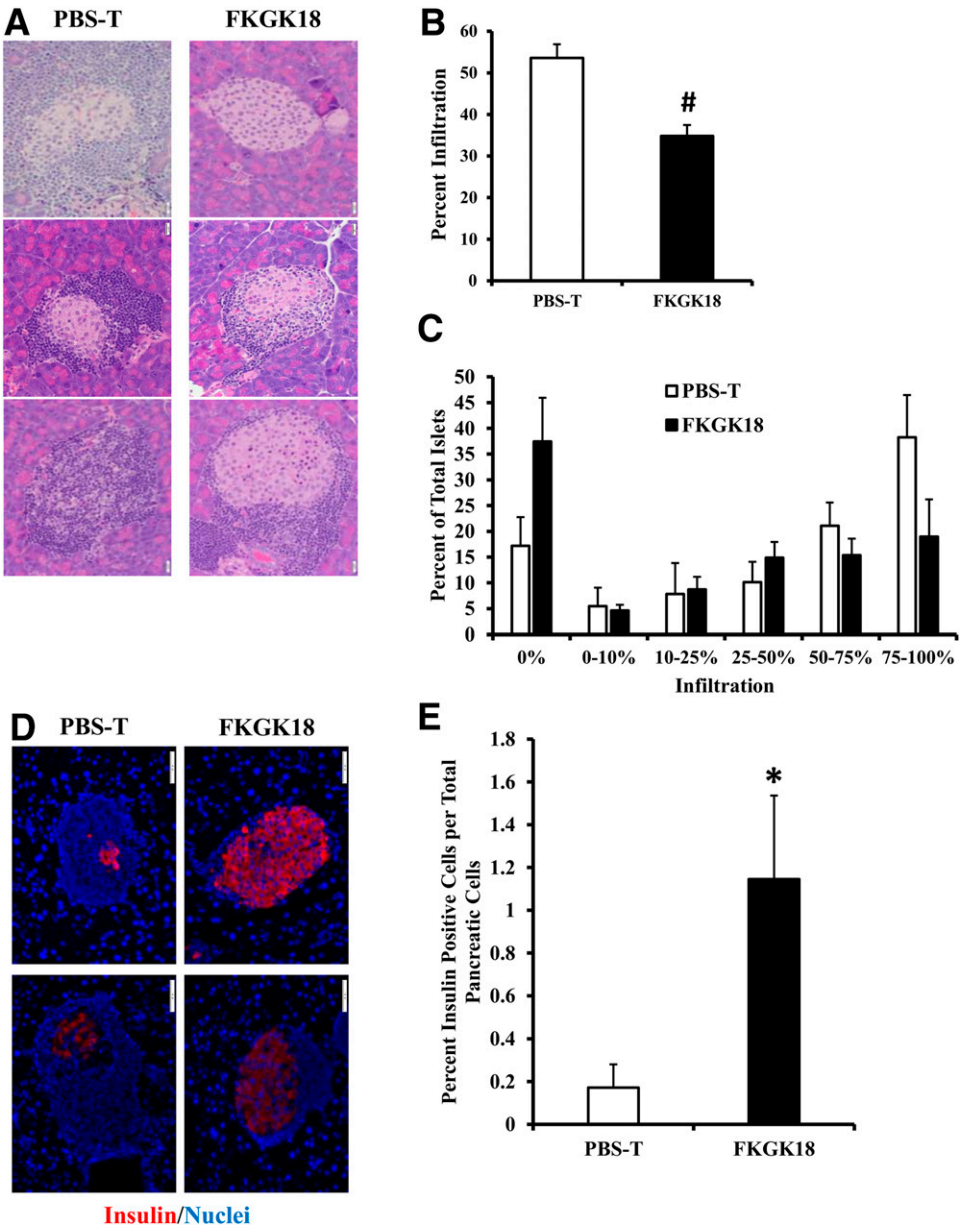

Figure 3—Islet infiltration and insulin staining. Mice were treated as described in Fig. 2. *A*: H-E staining of islets. Paraffin sections (10 μm) of pancreas sections prepared from the vehicle and FKGK18 groups were stained with H-E, and representative images (128 islets in 9 vehicle mice and 195 islets in 11 FKGK18 mice) are presented. Original magnification ×400, scale bar = 20 μm. *B*: Quantitation of islet infiltration. Percent infiltration for each islet was calculated as the value of noninfiltrated area subtracted from total islet area (% infiltrate = 100 × [(total area – noninfiltrate area) / (total area)]) using ImageJ software. Data are mean ± SEM of percent of islet infiltrated. #$P < 0.0001$, FKGK18 group vs. vehicle group (n = 128 vehicle islets and n = 195 FKGK18 islets). *C*: Insulitis spectrum. Distribution of percentage infiltration (0–100% relative to total islet area) among individual islets from vehicle (n = 128) and FKGK18 (n = 195) groups is presented as percent of total islets. *D* and *E*: Insulin staining area in sections. β-Cell area, as reflected by insulin staining, was calculated as percent of total pancreas area (% β-cells = 100 × [β-cell area sum per pancreas / pancreas area total]). Pancreas sections (from 9 vehicle and 11 FKGK18 mice) were stained for insulin (*D*), and the percent area of total insulin-containing stain relative to total pancreas area is presented as mean ± SEM (*E*). Original magnification ×400, scale bar = 50 μm. *$P < 0.05$, FKGK18 group vs. vehicle group. PBS-T, PBS + 5% Tween 80.

islets from both the vehicle and the FKGK18 groups. However, CD4$^+$ T cells and B cells per islet (Fig. 4*B* and *D*), but not CD8α$^+$ T cells (Fig. 4*C*), were significantly decreased in the FKGK18 group relative to the vehicle group, suggesting that islet infiltration by certain immune cells is impeded with inactivation of iPLA$_2$β.

NOD Immune Cells Express iPLA$_2$β, and FKGK18 Reduces CD4$^+$ T-Cell and B-Cell Function

PCR analyses revealed that NOD splenocytes, CD4$^+$ T cells, B cells, and bone marrow–derived macrophages all express iPLA$_2$β mRNA (Fig. 5*A*), raising the possibility that iPLA$_2$β activation affects their functionality. Initial studies revealed that FKGK18 exposure for up to 72 h

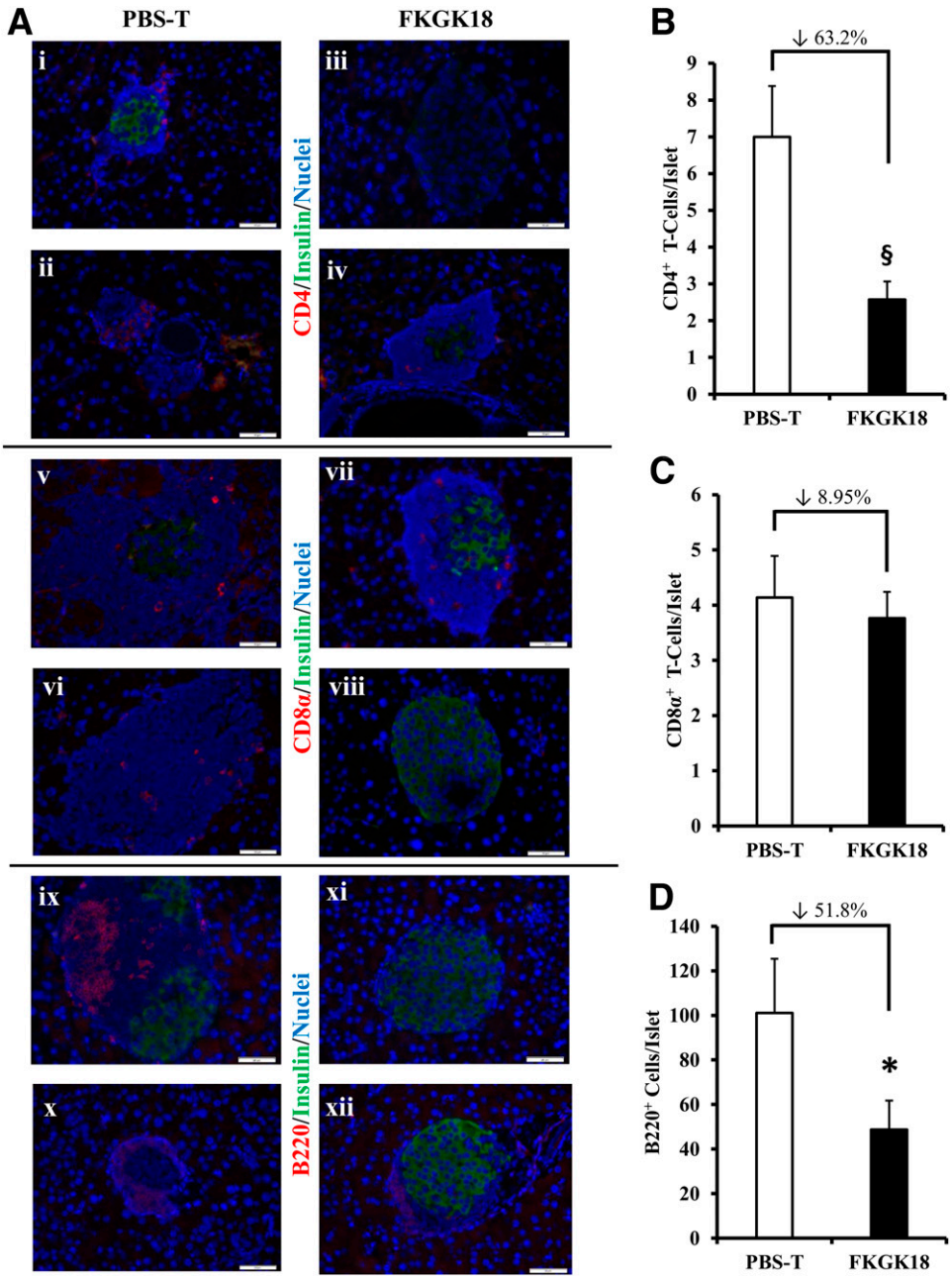

Figure 4—Immune cell phenotyping in islet infiltrates. Paraffin sections (10 μm) of pancreas prepared from mice treated with vehicle or FKGK18 were stained for $CD4^+$ and $CD8^+$ T cells or B cells. *A*: Representative images of islets from vehicle and FKGK18 groups stained separately for $CD4^+$ T cells (*i* and *ii*, *iii* and *iv*), $CD8\alpha^+$ T cells (*v* and *vi*, *vii* and *viii*), or B cells (B220, *ix* and *x*, *xi* and *xii*). Original magnification ×400, scale bar = 50 μm. Each image was obtained from a different mouse. The immune cell populations are visualized in red, insulin in green, and nuclei in blue. *B–D*: Quantitation of immune cell number per islet. Data reflecting analyses of islets from a minimum of five mice per group are presented as mean ± SEM of $CD4^+$ T cells (*B*, §$P < 0.001$; vehicle: 7 ± 1.38 cells/islet, $n = 50$; FKGK18: 2.57 ± 0.48 cells/islet, $n = 78$), $CD8\alpha^+$ T cells (*C*, not significant; vehicle: 4.13 ± 0.75 cells/islet, $n = 51$; FKGK18: 3.76 ± 0.47 cells/islet, $n = 85$), and $B220^+$ B cells (*D*, *$P < 0.05$; vehicle: 101.09 ± 24.30 cells/islet, $n = 52$; FKGK18: 48.71 ± 13.03 cells/islet, $n = 103$). PBS-T, PBS + 5% Tween 80.

does not compromise cell viability (Supplementary Figs. 1*A* and 2*A*) and reduces cytokine generation from mixed splenocytes but not macrophages (Supplementary Figs. 1*B–D* and 2*B–C*).

The effects of FKGK18 (10^{-7}–10^{-5} mol/L, 72 h) on $CD4^+$ T-cell and B-cell function were assessed next. Exposure of $CD4^+$ T cells, activated with αCD3 and αCD28 (31), to FKGK18 had no effect on cell viability (Fig. 5*B*) or generation of IFN-γ and IL-2 (Fig. 5*C*), but TNF-α generation was significantly decreased (Fig. 5*D*) relative to the vehicle group. In contrast, viability of B cells (Fig. 5*E*), activated by LPS + IL-4, was significantly reduced by FKGK18, paralleling decreases in both IgG and IgM production (Fig. 5*F*). However, FKGK18 (10^{-6} mol/L) caused an

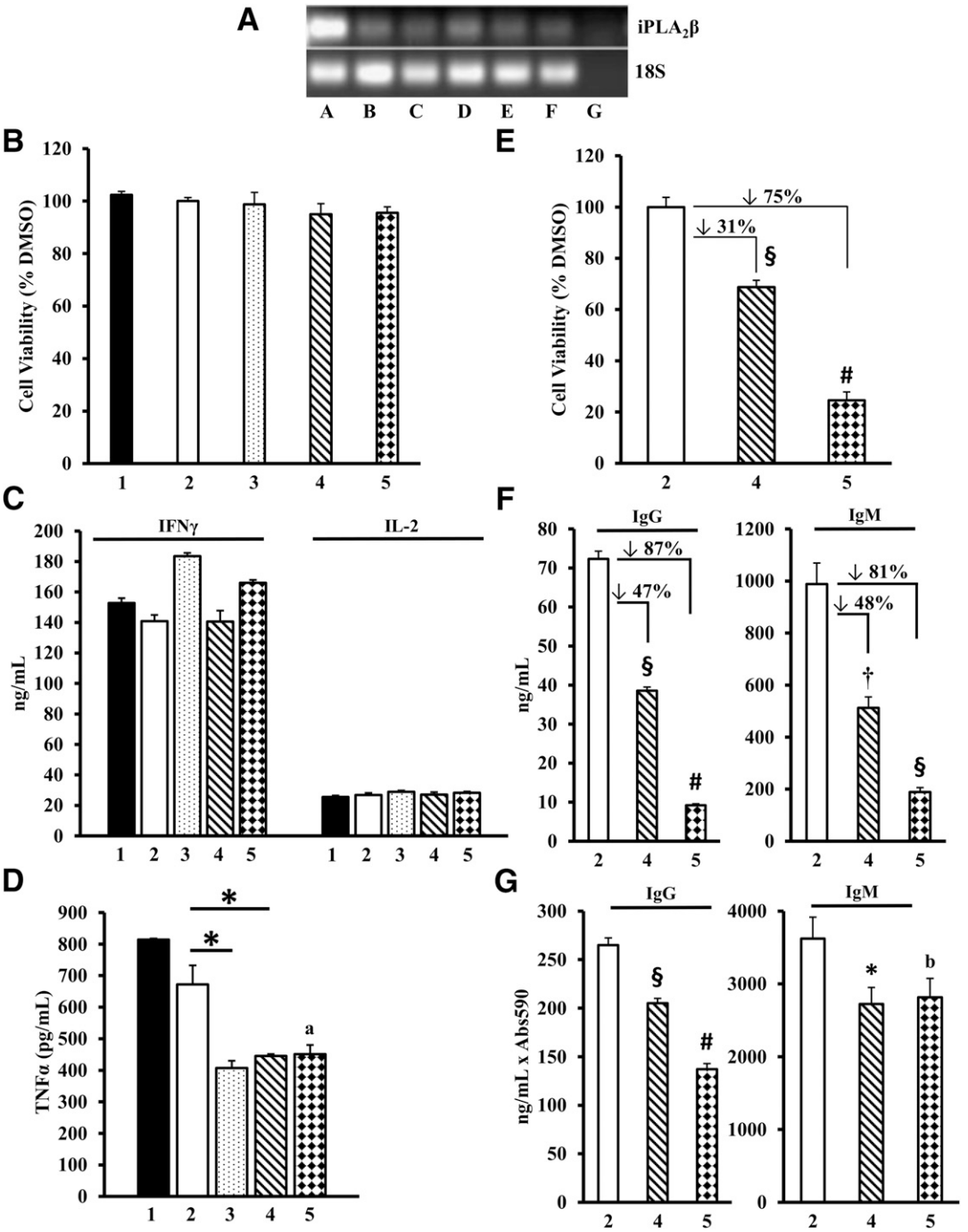

Figure 5—Viability of and cytokine production by CD4$^+$ T cells in the absence and presence of FKGK18. Immune cells were prepared from 8–12-week-old NOD female mice for iPLA$_2$β mRNA, viability (by MTT assay), and cytokine/immunoglobulin production (by ELISA) analyses. *A*: Expression of iPLA$_2$β. cDNA generated from RNA isolated from splenocytes, purified CD4$^+$ T cells and B cells, and bone marrow–derived macrophages were used for iPLA$_2$β message analyses by RT-PCR (*lane A*, positive control brain; *lane B*, splenocytes; *lane C*, CD4$^+$ T cells; *lane D*, B cells; *lane E*, bone marrow–derived macrophages; *lane F*, islets; *lane G*, no template control). *B*: CD4$^+$ T-cell viability. Viability of cells in each well after removal of medium was assessed by MTT assay, and absorbance at 590 nm, reflecting the number of viable cells, is presented as percent of DMSO vehicle. *C* and *D*: Production of IFN-γ, IL-2, and TNF-α ± FKGK18. Media were collected at 72 h, and cytokine contents were determined by ELISA. *P < 0.05, FKGK18 group vs. DMSO group; $^a P$ = 0.07, condition 5 vs. +DMSO (n = 3). *E–G*: B cells were treated with 1 μg/mL LPS + 2 ng/mL IL-4 for 72 h ± FKGK18. *E*: Viability was assessed by MTT assay and presented as percent of DMSO vehicle. §P < 0.0005 vs. +DMSO; #P < 0.00005 vs. +DMSO (n = 5). *F*: Antibody production. IgG and IgM in the media were determined by ELISA and presented as mean ± SEM. §P < 0.0005 vs. +DMSO; #P < 0.00005 vs. +DMSO; †P < 0.005 vs. +DMSO (n = 4). *G*: Antibody production per cell. IgG and IgM concentrations were normalized to viable cells, as reflected by MTT absorbance at 590 nm, and presented as mean ± SEM. §P < 0.0005 vs. +DMSO; #P < 0.00005 vs. +DMSO; *P < 0.05 vs. +DMSO; $^b P$ = 0.09, condition 5 vs. +DMSO (n = 4). Condition 1, −DMSO; condition 2, +DMSO; condition 3, 10^{-7} mol/L FKGK18; condition 4, 10^{-6} mol/L FKGK18; condition 5, 10^{-5} mol/L FKGK18.

~20% greater reduction in antibody production compared with its effects on cell viability. Moreover, significant decreases in both were still evident when antibody production was normalized to cell viability (Fig. 5*G*). These findings suggest that sensitivity of different immune cells to $iPLA_2\beta$ varies and that in addition to affecting immune cell function, $iPLA_2\beta$ activation may influence B-cell survival/proliferation.

$CD4^+$ T-Cell Function Is Mediated by β-Isoform of $iPLA_2$

To verify that the in vivo effects of FKGK18 are due to $iPLA_2\beta$ inhibition, the effects of FKGK18, *S*-BEL (specific for $iPLA_2\beta$), and *R*-BEL (specific for $iPLA_2\gamma$) were compared. Cell viability with vehicle and FKGK18 exposures was similar between 24 and 72 h, suggesting that proliferation of cells was not compromised by FKGK18 (Fig. 6*A*). $CD4^+$ T

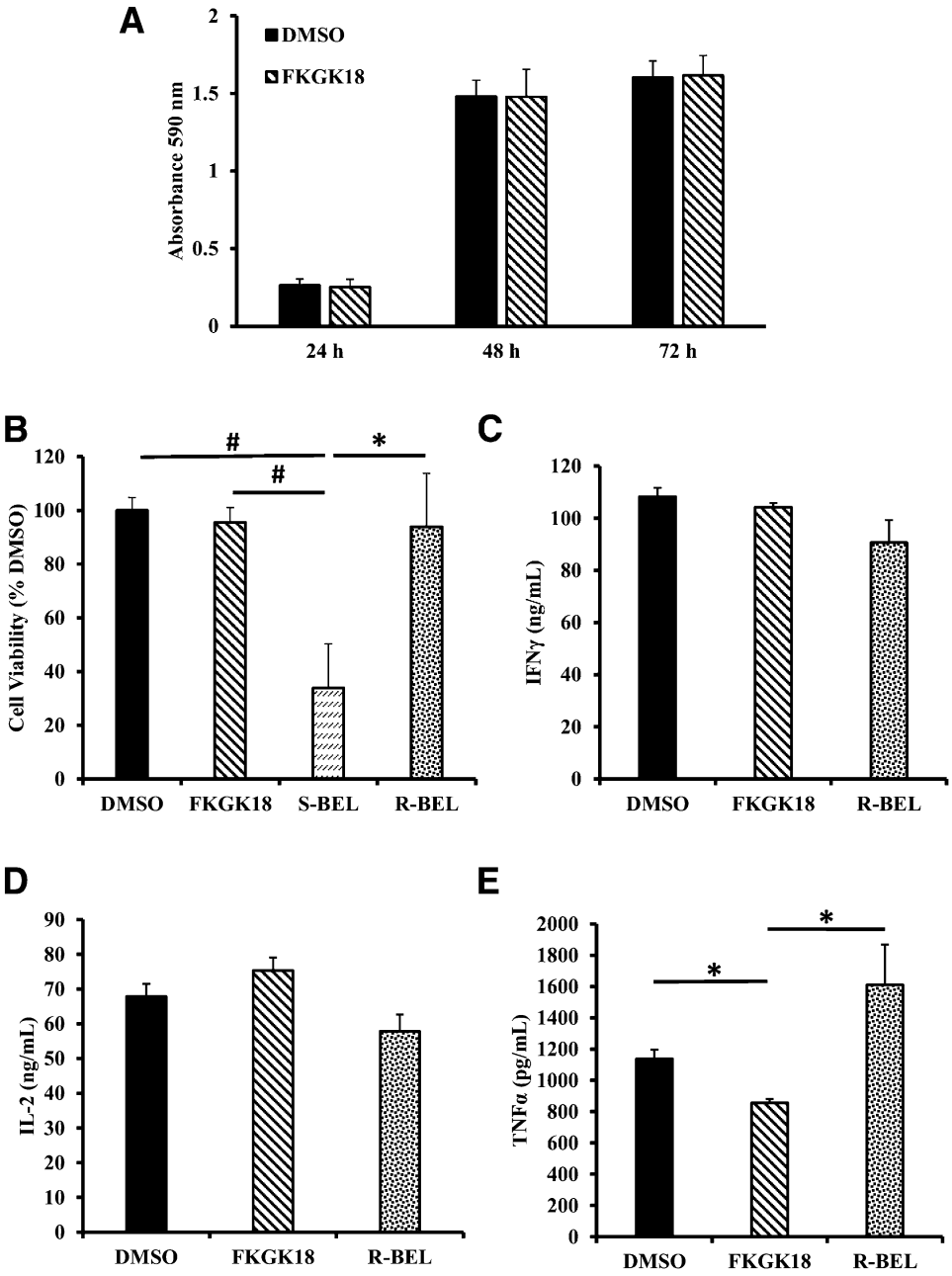

Figure 6—Comparison of FKGK18 vs. $iPLA_2$ inhibitors on viability and cytokine production in $CD4^+$ T cells. Purified $CD4^+$ T cells from 8–12-week-old NOD mice were treated with vehicle alone (DMSO) or $iPLA_2$ inhibitors (FKGK18, 10^{-6} mol/L; *S*-BEL, 10^{-5} mol/L; *R*-BEL, 10^{-5} mol/L) for 72 h. *A*: $CD4^+$ T-cell proliferation. Viability of cells in each well after removal of medium was assessed by MTT assay and absorbance at 590 nm, reflecting the number of viable cells, and is presented as a function of FKGK18 (10^{-6} mol/L) exposure time. *B*: Cell viability. Viability assessed, as described in Fig. 5, is presented as percent of DMSO vehicle. #$P < 0.0001$, *S*-BEL group vs. DMSO and FKGK18 groups; *$P < 0.05$, *S*-BEL group vs. *R*-BEL group ($n = 3$). *C–E*: Cytokine production. IFN-γ (*C*), IL-2 (*D*), and TNF-α (*E*) measured in the media by ELISA are presented as mean ± SEM. *$P < 0.05$, FKGK18 group vs. other groups ($n = 3$).

cells were then exposed to *S*-BEL or *R*-BEL for only 30 min (4,5), unlike FKGK18, which was present for the entire 72 h. Similar to FKGK18, viability of CD4$^+$ T cells (Fig. 6*B*) or IFN-γ (Fig. 6*C*) and IL-2 (Fig. 6*D*) production were not affected by *R*-BEL. However, unlike FKGK18, *R*-BEL did not inhibit TNF-α generation (Fig. 6*E*). In contrast, cell viability was significantly reduced by *S*-BEL (Fig. 6*B*), and cytokine generation was barely detectable (data not shown). These findings suggest that the in vivo effects of FKGK18 were due to inhibition of iPLA$_2$β and not iPLA$_2$γ.

Effects of Eicosanoid Inhibitors on CD4$^+$ T Cells

Because CD4$^+$ T cells and TNF-α are critical mediators of diabetes development and we found that they are affected by iPLA$_2$β activation, the effects of inhibiting eicosanoid generation on TNF-α production from CD4$^+$ T cells was examined. The cells were exposed to inhibitors of COX (indomethacin), LOX (nordihydroguaiaretic acid [NDGA]), COX and LOX (5,8,11,14-eicosatetraynoic acid [ETYA]), or 12-LOX (cinnamyl-3,4-dihydroxy-α-cyanocinnamate [CDC]). In the absence of compromising cell viability (Fig. 7*A*), indomethacin, ETYA, and CDC mimicked FKGK18 inhibition of TNF-α production, but NDGA at concentrations <10 μmol/L, which inhibit 5-LOX but not 12-LOX, had no effect (Fig. 7*B*) relative to vehicle treatment. These findings provide evidence for participation of iPLA$_2$β-derived lipids generated by COX and 12-LOX in modulating immune cell function. This is supported by decreased PGE$_2$ generation with FKGK18, analogous to the COX inhibitors (Fig. 7*C*).

Adoptive Transfer of Type 1 Diabetes

Given this evidence for iPLA$_2$β-derived lipid involvement in modulating CD4$^+$ T-cell function, we examined the ability of FKGK18 to inhibit adoptive transfer of diabetes to immunodeficient NOD.*scid* mice by CD4$^+$ T cells. Consistent with unchanged blood glucose levels (Fig. 8*A*), there was no evidence of diabetes development in untreated control and vehicle- or FKGK18 alone–treated mice (Fig. 8*B*). However, diabetes incidence was nearly 90% in mice following administration of CD4$^+$ T cells (Fig. 8*B*). In contrast, the incidence was significantly reduced to ~40% in mice that were pretreated for 1 week with FKGK18 before CD4$^+$ T-cell transfer. In comparison, initiation of FKGK18 treatment at the time of transfer or administration of cells pretreated with FKGK18 for 3 days was without protective effect (Fig. 8*C*).

DISCUSSION

Type 1 diabetes is a consequence of autoimmune destruction of β-cells, and there is increasing evidence of iPLA$_2$β induction in diabetes and for its participation in β-cell apoptosis (3–6,13–15,32). We therefore considered the possibility that inhibition of iPLA$_2$β mitigates β-cell death and ameliorates diabetes development. Consistent with this, we found that iPLA$_2$β expression in islets from prediabetic female NOD mice is much higher than in diabetes-resistant mice. FK-based inhibitors with variable specificity for iPLA$_2$β have proven to be effective in countering central nervous system–related disorders (20–22). Our characterization of FKGK18 (19), which exhibits greater specificity for iPLA$_2$β over other PLA$_2$s (7,18,33), revealed FKGK18 to be more specific for iPLA$_2$β than iPLA$_2$γ and in contrast to BEL (9,16), to not inhibit other serine proteases.

The NOD mouse is a model of spontaneous type 1 diabetes development, and as expected (30), ~80% of the female NOD mice developed diabetes by 25 weeks of age. In contrast, FKGK18 administration started at 10 days of age significantly reduced diabetes incidence. Concomitant observations included decreases in islet infiltration by immune cells, higher levels of circulating insulin, preservation of β-cell area, and improved glucose homeostasis. Together, these findings suggest that inhibiting iPLA$_2$β may be effective in ameliorating diabetes evolution.

Mass spectrometry protocols revealed that FKGK18 levels in the serum were maximum by 2–6 h but near minimal by 48 h, implying that the current regimen (three times per week) would not be expected to lead to significant accumulations of the inhibitor, therefore limiting its toxicity. Consistent with this, mice receiving FKGK18 exhibited similar body weights over 30 weeks, no discernible damage in nonislet tissues, prolonged euglycemia, and consequential survival. Taken together, these observations indicate that the FKGK18 regimen used does not promote systemic toxicity and is well tolerated.

The reversible nature of FKGK18 precludes measurement of iPLA$_2$β activity following tissue isolation, requiring an alternate measure of iPLA$_2$β inhibition in vivo. Both *S*-BEL (34,35) and FKGK18 (19) decrease PGE$_2$ release from pancreatic islets; however, PGE$_2$ is metabolized further in vivo and thus is an unreliable measure of PLA$_2$ activity. We therefore measured urinary PGEM levels and found them to be decreased by ~25% for up to 42 h following FKGK18 administration but returned to control levels beyond 48 h, consistent with its bioavailability. Given its specificity for iPLA$_2$β over other PLA$_2$s (18,19), these observations are taken as a reflection of reversible inhibition of iPLA$_2$β by FKGK18. Because urine was collected from chronically treated mice, the continued generation of PGEMs suggests that activities of other PLA$_2$s are not compromised by FKGK18.

Remarkably, FKGK18 dramatically reduced insulitis. Infiltration of islets by immune cells is a precursor event that leads to β-cell destruction (30), and CD4$^+$ T cells and B cells, which independently and in concert destroy β-cells (36), were reduced by FKGK18. These findings suggest that FKGK18 may impede immune cell migration into or proliferation within the islet. With evidence of iPLA$_2$β mRNA expression in immune cells, we considered the possibility that CD4$^+$ T-cell and B-cell functionality also is affected by FKGK18. Because of their importance to the development of diabetes (37), we examined whether generation of proinflammatory cytokines by immune cells from NOD mice is altered in the presence of

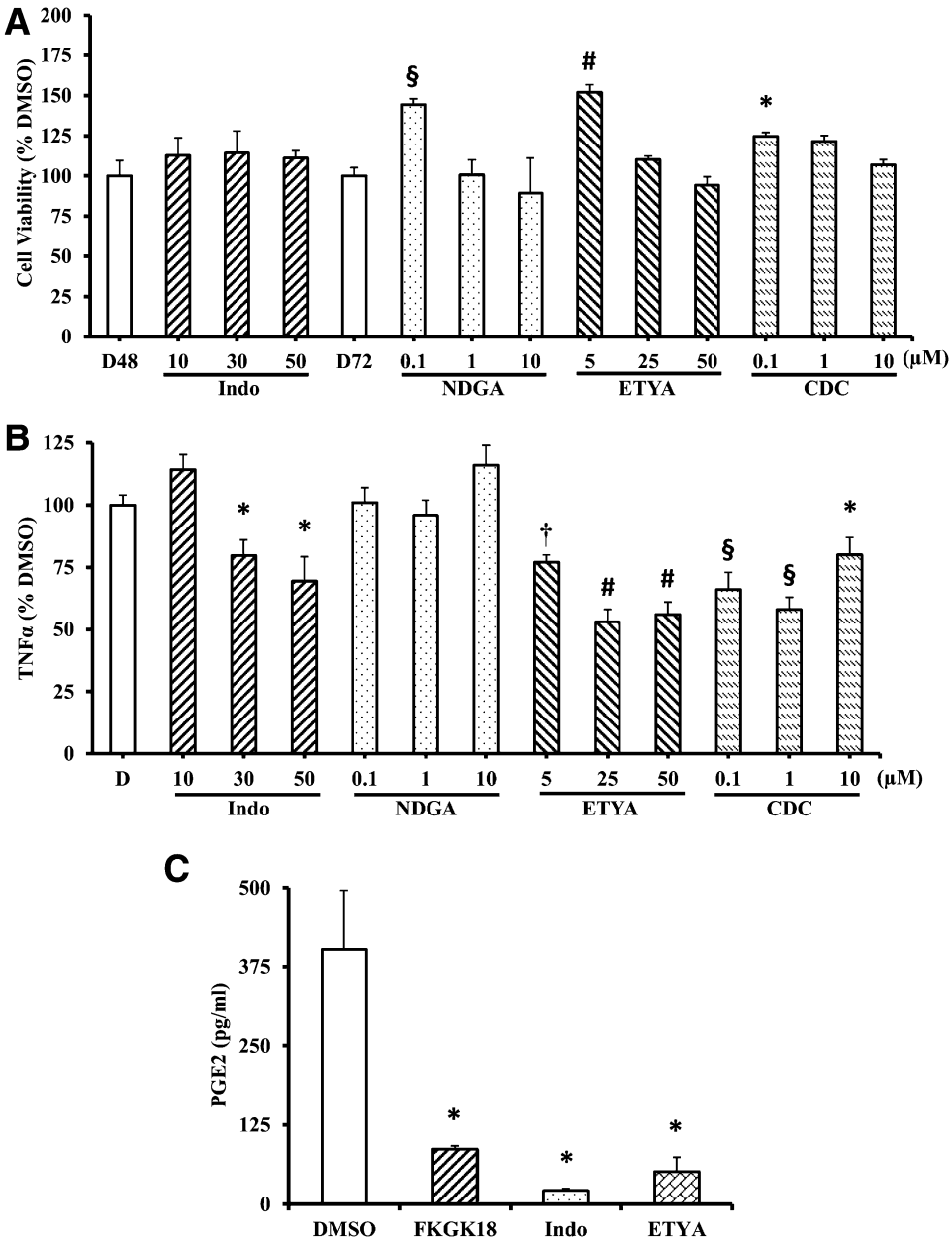

Figure 7—Effects of eicosanoid inhibitors on $CD4^+$ T cells. $CD4^+$ T cells purified from 8–12-week-old NOD female mice were treated with DMSO alone or with inhibitors of COX2 (indomethacin [Indo] 10–50 μmol/L, 48 h); 5-LOX and 12-LOX (NDGA 1–10 μmol/L, 72 h); COX and LOX (ETYA 5–50 μmol/L, 72 h); or 12-LOX (CDC 0.1–10 μmol/L, 72 h). *A*: Cell viability. Viability assessed, as described in Fig. 5, is presented as mean ± SEM. §$P < 0.001$ vs. D72 group; #$P < 0.0001$ vs. D72 group; *$P < 0.05$ vs. D72 group (n = 5–25). *B*: TNF-α production. TNF-α in the media was determined by ELISA and presented as percent of DMSO vehicle. *$P < 0.05$ vs. DMSO group; †$P < 0.005$ vs. DMSO group; #$P < 0.0001$ vs. DMSO group; §$P < 0.001$ vs. DMSO group (n = 5–25). *C*: PGE_2 generation. The PGE_2 generation in the presence of FKGK18 (10^{-6} mol/L) was compared with the COX inhibitors (indomethacin 30 μmol/L, ETYA 50 μmol/L). Medium from $CD4^+$ T cells was collected at the end of the inhibitor regimen, and PGE_2 content was determined by ELISA and presented as mean ± SEM. *$P < 0.05$ vs. DMSO group (n = 3).

prototypical stimulants. Generation of IFN-γ and IL-2 by splenocytes with concanavalin A and of the chemoattractant TNF-α (38) by $CD4^+$ T cells with αCD3/αCD28 was reduced by FKGK18. These differences are likely due to splenocytes being an admixture of leukocytes, with the bulk being B cells and only ~10% $CD4^+$ T cells. In contrast, macrophages exposed to LPS were unaffected by FKGK18, analogous to the inability of zymosan to alter arachidonate release from macrophages treated with $iPLA_2\beta$ inhibitors (39) or from $iPLA_2\beta$-deficient mice (40). The lack of effects in macrophages under the conditions tested is further evidence for the absence of nonspecific effects of FKGK18. Consistent with this, *R*-BEL, which is specific for the membrane-associated

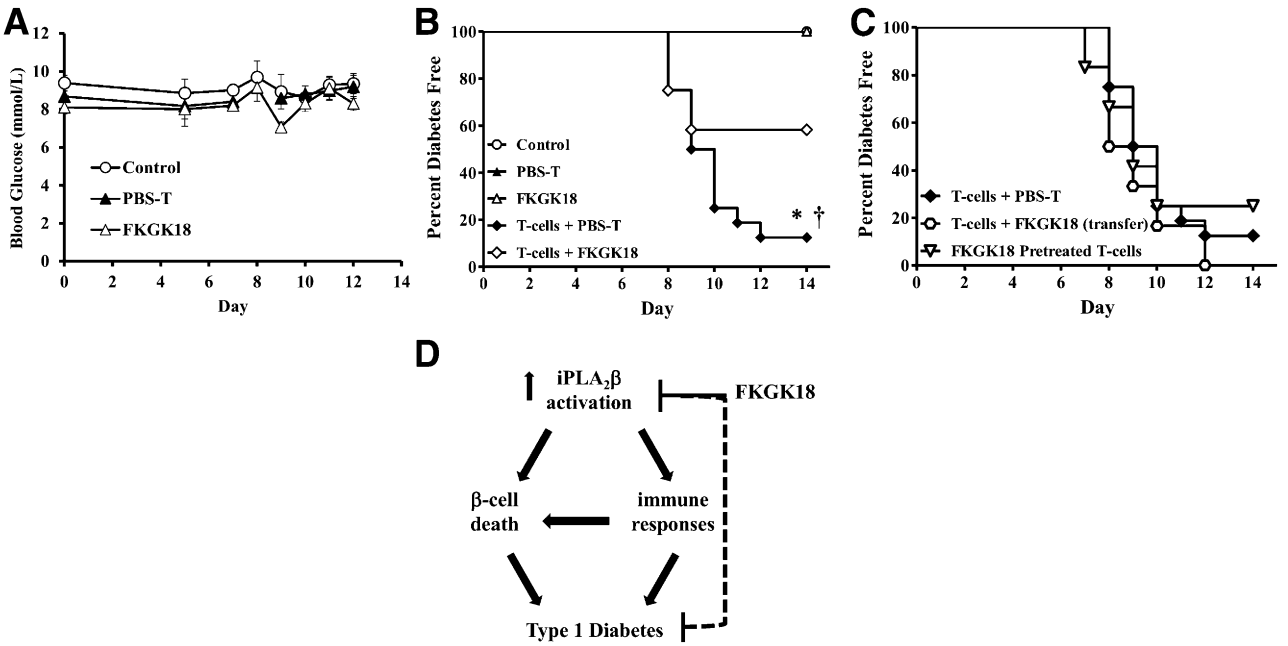

Figure 8—Adoptive transfer of diabetes to immunodeficient NOD.*scid* mice. CD4$^+$ T cells were purified from 12-week-old male BDC2.5/NOD mice (activated with αCD3 and αCD28 and expanded with IL-2) before transfer. Six-week-old male diabetes-resistant NOD.*scid* mice were divided into three groups: untreated (control), vehicle (PBS + 5% Tween 80 [PBS-T]), and FKGK18 alone (20 mg/kg i.p.). After 1 week, the vehicle group was either maintained with vehicle (n = 13) or administered T cells (100 μL HBSS i.p., 5×10^5 cells/mouse) + vehicle (n = 16), T cells + FKGK18 (n = 12), or T cells pretreated with FKGK18 (10^{-6} mol/L for 3 days) (n = 12). The FKGK18 group was either maintained with FKGK18 (n = 6) or administered T cells (n = 12). Once initiated, FKGK18 was administered every 48 h (20 mg/kg i.p.) until the end of the study. Blood glucose was monitored over a 14-day period to identify diabetes onset (≥15.3 mmol/L). *A*: Blood glucose in control groups. Blood glucose levels in control, PBS-T alone, and FKGK18 alone groups. *B*: Diabetes incidence in control, PBS-T alone, FKGK18 alone, T cells + vehicle, and T cells + FKGK18 pretreated groups. *P < 0.05 vs. T cells alone group; †P < 0.005 vs. T cells alone group. *C*: Diabetes incidence in T cells + vehicle, FKGK18-pretreated T cells, and T cells + FKGK18 administered at the same time groups. *D*: Proposed model of iPLA$_2$β role in the development of type 1 diabetes. Our earlier work suggested that iPLA$_2$β participates in β-cell apoptosis through the induction of ceramide generation from hydrolysis of sphingomyelins, triggering the intrinsic apoptotic pathway (3,4,6,48). The current findings reveal an additional impact of iPLA$_2$β activation on immune responses. We suggest that iPLA$_2$β-derived lipid signals contribute to β-cell destruction and consequential diabetes development partly through these mechanisms and that inactivation of iPLA$_2$β may be beneficial in ameliorating type 1 diabetes.

iPLA$_2$γ (16), did not inhibit TNF-α production from CD4$^+$ T cells.

Although their precise role has not yet been clearly defined, B cells are recognized to be critical to the development of type 1 diabetes (41,42), and antibody production by B cells was reduced by FKGK18. Of all the immune cells, only B-cell viability was significantly diminished by FKGK18, suggesting differential sensitivity of these cells to iPLA$_2$β inhibition. This in combination with decreased infiltrate CD4$^+$ T cells, which stimulate B-cell proliferation, may account for the reductions in B cells in the islet infiltrate.

These observations suggest that modulation of immune cell function may be a mechanism by which iPLA$_2$β-derived lipid signals participate in autoimmune β-cell death. Recognizing the critical role of T cells and TNF-α in diabetes development, the effects of eicosanoid-generating pathway inhibitors on TNF-α production by CD4$^+$ T cells were examined. Such analyses revealed that the inhibition of TNF-α production by FKGK18 was mimicked by inhibitors of COX (indomethacin), COX and LOX (ETYA), and 12-LOX (CDC) but unaffected by the LOX inhibitor NDGA (at a concentration range that inhibits 5-LOX but not 12-LOX). These findings suggest that lipid signals generated by COX and 12-LOX, subsequent to iPLA$_2$β-mediated hydrolysis of arachidonic acid, are likely candidate modulators of immune cell function. Consistent with this, FKGK18 inhibited PGE$_2$ generation by the CD4$^+$ T cells analogous to the COX inhibitors. Contribution of COX and 12-LOX products to the autoimmune responses is supported by reports that PGE$_2$ release is significantly higher from NOD islets that are infiltrated versus non-infiltrated (43) and that deletion of 12/15-LOX protects against diabetes development (44). Further analyses using specific inhibitors of the eicosanoid-generating pathways are expected to more definitively identify the relevant eicosanoids.

The role for iPLA$_2$β-derived lipid signals in type 1 diabetes development is strengthened by the findings that adoptive transfer of diabetes to NOD.*scid* mice, which are immunodeficient and diabetes resistant, by CD4$^+$ T cells is mitigated by pretreatment of the mice with FKGK18. However, administration of T cells and FKGK18 simultaneously was ineffective in mitigating diabetes development,

suggesting that in vivo, $iPLA_2\beta$ activation permits immune cell responses and that to counter this effect, $iPLA_2\beta$ inhibition must occur before islet onslaught by immune cells. Furthermore, no protection from diabetes development could be demonstrated with transfer of FKGK18-pretreated T cells, and this most likely reflects the reversible nature of FKGK18 and its limited bioavailability beyond 3 days.

Although we found that inhibiting $iPLA_2\beta$ may be beneficial in mitigating type 1 diabetes evolution, its participation in multiple biological processes (9) presents the potential for deleterious consequences with global $iPLA_2\beta$ inhibition. It has been proposed that $iPLA_2\beta$ plays a housekeeping role to generate substrates for reincorporation into phospholipids. However, several lines of investigation have suggested that modulation of $iPLA_2\beta$ does not affect membrane phospholipids in islets or other tissues (45,46); thus, FKGK18 is not expected to alter membrane lipid composition. We and others have described a signal transduction role for $iPLA_2\beta$, including its amplification of glucose-stimulated insulin secretion (35,47). That it is counterintuitive to inhibit $iPLA_2\beta$ to achieve euglycemia, however, is allayed by the observations that *1)* $iPLA_2\beta$ is increased, not decreased, in diabetes-prone mice; *2)* fasting blood glucose levels in FKGK18-treated mice are not elevated relative to vehicle-treated NOD mice; *3)* circulating levels of insulin are higher in the FKGK18 group; and *4)* glucose tolerance is improved in the FKGK18 group in contrast to abnormal glucose tolerance in $iPLA_2\beta$-deficient mice (47).

In summary, chronic inhibition of $iPLA_2\beta$ with FKGK18 preserves β-cell mass and reduces autoimmune type 1 diabetes incidence (Fig. 8*D*). With evidence for $iPLA_2\beta$ expression in NOD β-cells and immune cells and for mitigation of immune cell function with $iPLA_2\beta$ inhibition, we suggest that lipids derived from β-cell or immune cell $iPLA_2\beta$ activation play critical signaling roles to promote recruitment, infiltration, or function of immune cells and that inhibition of $iPLA_2\beta$ may be beneficial in ameliorating diabetes.

Acknowledgments. The authors thank the University of Alabama at Birmingham (UAB) Comparative Pathology Laboratory and Trenton R. Schoeb (professor of genetics, UAB) for interpretation of histopathologic changes in non-islet tissues; Scott M. Tanner (postdoctoral fellow, Department of Surgery, UAB), Joseph G. Daft (PhD candidate, Department of Pathology, UAB), and Lindsey E. Padgett (PhD candidate, Department of Microbiology, UAB) for immune cell experimental protocols and advice; Lionel C. Clement (assistant professor of nephrology, UAB) and Sumant S. Chugh (professor of nephrology, UAB) for assistance with the urine collection protocol; and Edward A. Dennis (professor of chemistry, biochemistry, and pharmacology, University of California, San Diego) for constructive comments and advice.

Funding. This work was made possible by funds provided by the National Institutes of Health (R01-DK-69455), American Diabetes Association (1-09-RA-147), and the Iacocca Family Foundation and the support of the UAB Comprehensive Diabetes Center Beta Cell Biology Core and the Diabetes Research Center.

Duality of Interest. No conflicts of interest relevant to the article were reported.

Author Contributions. R.N.B. contributed to the design, experimentation, data analyses, and manuscript preparation and editing. Y.G. contributed to the design and experimentation. V.M. and G.K. contributed to the synthesis and characterization of FKGK18, data analyses, and manuscript preparation and editing. M.G.K. contributed to the high-resolution mass spectrometry protocol development and analyses for FKGK18 and mass spectrometry spectra. T.A. contributed to the characterization of FKGK18 and manuscript editing. X.L. contributed to the experimentation, data analyses, and manuscript editing. H.M.T. and S.R. contributed to the design, data analyses, and manuscript preparation and editing. S.R. is the guarantor of this work and, as such, had full access to all the data in the study and takes responsibility for the integrity of the data and the accuracy of the data analysis.

Prior Presentation. Parts of this study were presented in abstract form at the 73rd Scientific Sessions of the American Diabetes Association, Chicago, IL, 21–25 June 2013; the 74th Scientific Sessions of the American Diabetes Association, San Francisco, CA, 13–17 June 2014; the 5th International Conference on Phospholipase A2 Mediated Signaling in Translational Medicine, New Orleans, LA, 20–21 May 2013; the 13th International Conference on Bioactive Lipids in Cancer, Inflammation and Related Diseases, San Juan, Puerto Rico, 3–6 November 2013; and the 48th Annual Southeastern Regional Lipid Conference, Cashiers, NC, 13–15 November 2013. In all these cases, only a very general description of the data were included in abstracts of <250 words.

References

1. Atkinson MA, Maclaren NK. The pathogenesis of insulin-dependent diabetes mellitus. N Engl J Med 1994;331:1428–1436
2. Padgett LE, Broniowska KA, Hansen PA, Corbett JA, Tse HM. The role of reactive oxygen species and proinflammatory cytokines in type 1 diabetes pathogenesis. Ann N Y Acad Sci 2013;1281:16–35
3. Lei X, Bone RN, Ali T, et al. Genetic modulation of islet β-cell $iPLA_2\beta$ expression provides evidence for its impact on β-cell apoptosis and autophagy. Islets 2013;5:29–44
4. Lei X, Zhang S, Bohrer A, Barbour SE, Ramanadham S. Role of calcium-independent phospholipase $A_{(2)}\beta$ in human pancreatic islet β-cell apoptosis. Am J Physiol Endocrinol Metab 2012;303:E1386–E1395
5. Ramanadham S, Hsu FF, Zhang S, et al. Apoptosis of insulin-secreting cells induced by endoplasmic reticulum stress is amplified by overexpression of group VIA calcium-independent phospholipase A_2 ($iPLA_2$ β) and suppressed by inhibition of $iPLA_2$ β. Biochemistry 2004;43:918–930
6. Lei X, Bone RN, Ali T, et al. Evidence of contribution of $iPLA_2\beta$-mediated events during islet β-cell apoptosis due to proinflammatory cytokines suggests a role for $iPLA_2\beta$ in T1D development. Endocrinology 2014;155:3352–3364
7. Dennis EA, Cao J, Hsu YH, Magrioti V, Kokotos G. Phospholipase A_2 enzymes: physical structure, biological function, disease implication, chemical inhibition, and therapeutic intervention. Chem Rev 2011;111:6130–6185
8. Gijón MA, Leslie CC. Phospholipases A_2. Semin Cell Dev Biol 1997;8:297–303
9. Wilkins WP 3rd, Barbour SE. Group VI phospholipases A_2: homeostatic phospholipases with significant potential as targets for novel therapeutics. Curr Drug Targets 2008;9:683–697
10. Gross RW, Ramanadham S, Kruszka KK, Han X, Turk J. Rat and human pancreatic islet cells contain a calcium ion independent phospholipase A_2 activity selective for hydrolysis of arachidonate which is stimulated by adenosine triphosphate and is specifically localized to islet beta-cells. Biochemistry 1993;32:327–336
11. Nanda BL, Nataraju A, Rajesh R, Rangappa KS, Shekar MA, Vishwanath BS. PLA2 mediated arachidonate free radicals: PLA2 inhibition and neutralization of free radicals by anti-oxidants—a new role as anti-inflammatory molecule. Curr Top Med Chem 2007;7:765–777
12. Weaver JR, Holman TR, Imai Y, et al. Integration of pro-inflammatory cytokines, 12-lipoxygenase and NOX-1 in pancreatic islet beta cell dysfunction. Mol Cell Endocrinol 2012;358:88–95
13. Ayilavarapu S, Kantarci A, Fredman G, et al. Diabetes-induced oxidative stress is mediated by Ca^{2+}-independent phospholipase A_2 in neutrophils. J Immunol 2010;184:1507–1515

14. Rahnema P, Shimoni Y, Nygren A. Reduced conduction reserve in the diabetic rat heart: role of iPLA$_2$ activation in the response to ischemia. Am J Physiol Heart Circ Physiol 2011;300:H326–H334
15. Xie Z, Gong MC, Su W, Xie D, Turk J, Guo Z. Role of calcium-independent phospholipase A$_2$β in high glucose-induced activation of RhoA, Rho kinase, and CPI-17 in cultured vascular smooth muscle cells and vascular smooth muscle hypercontractility in diabetic animals. J Biol Chem 2010;285:8628–8638
16. Jenkins CM, Han X, Mancuso DJ, Gross RW. Identification of calcium-independent phospholipase A$_2$ (iPLA$_2$) beta, and not iPLA$_2$gamma, as the mediator of arginine vasopressin-induced arachidonic acid release in A-10 smooth muscle cells. Enantioselective mechanism-based discrimination of mammalian iPLA$_2$s. J Biol Chem 2002;277:32807–32814
17. Fuentes L, Pérez R, Nieto ML, Balsinde J, Balboa MA. Bromoenol lactone promotes cell death by a mechanism involving phosphatidate phosphohydrolase-1 rather than calcium-independent phospholipase A$_2$. J Biol Chem 2003;278:44683–44690
18. Kokotos G, Hsu YH, Burke JE, et al. Potent and selective fluoroketone inhibitors of group VIA calcium-independent phospholipase A$_2$. J Med Chem 2010;53:3602–3610
19. Ali T, Kokotos G, Magrioti V, et al. Characterization of FKGK18 as inhibitor of group VIA Ca^{2+}-independent phospholipase A$_2$ (iPLA$_2$β): candidate drug for preventing beta-cell apoptosis and diabetes. PLoS One 2013;8:e71748
20. Kalyvas A, Baskakis C, Magrioti V, et al. Differing roles for members of the phospholipase A2 superfamily in experimental autoimmune encephalomyelitis. Brain 2009;132:1221–1235
21. López-Vales R, Ghasemlou N, Redensek A, et al. Phospholipase A$_2$ superfamily members play divergent roles after spinal cord injury. FASEB J 2011;25:4240–4252
22. López-Vales R, Navarro X, Shimizu T, et al. Intracellular phospholipase A(2) group IVA and group VIA play important roles in Wallerian degeneration and axon regeneration after peripheral nerve injury. Brain 2008;131:2620–2631
23. Li H, Zhao Z, Antalis C, et al. Combination therapy of an inhibitor of group VIA phospholipase A$_2$ with paclitaxel is highly effective in blocking ovarian cancer development. Am J Pathol 2011;179:452–461
24. Kim SH, Kook MC, Song HG. Optimal conditions for the retrieval of CD4 and CD8 antigens in formalin-fixed, paraffin-embedded tissues. J Mol Histol 2004;35:403–408
25. Zhang Y, Zhang Y, Bone RN, et al. Regeneration of pancreatic non-β endocrine cells in adult mice following a single diabetes-inducing dose of streptozotocin. PLoS One 2012;7:e36675
26. Tse HM, Milton MJ, Schreiner S, Profozich JL, Trucco M, Piganelli JD. Disruption of innate-mediated proinflammatory cytokine and reactive oxygen species third signal leads to antigen-specific hyporesponsiveness. J Immunol 2007;178:908–917
27. Bondada S, Robertson DA. Assays for B lymphocyte function. Curr Protoc Immunol 2003;56(II:3.8):3.8.1–3.8.24
28. Staley EM, Schoeb TR, Lorenz RG. Differential susceptibility of P-glycoprotein deficient mice to colitis induction by environmental insults. Inflamm Bowel Dis 2009;15:684–696
29. Haskins K, Portas M, Bergman B, Lafferty K, Bradley B. Pancreatic islet-specific T-cell clones from nonobese diabetic mice. Proc Natl Acad Sci U S A 1989;86:8000–8004
30. Anderson MS, Bluestone JA. The NOD mouse: a model of immune dysregulation. Annu Rev Immunol 2005;23:447–485
31. Riddell SR, Greenberg PD. The use of anti-CD3 and anti-CD28 monoclonal antibodies to clone and expand human antigen-specific T cells. J Immunol Methods 1990;128:189–201
32. Lei X, Zhang S, Barbour SE, et al. Spontaneous development of endoplasmic reticulum stress that can lead to diabetes mellitus is associated with higher calcium-independent phospholipase A$_2$ expression: a role for regulation by SREBP-1. J Biol Chem 2010;285:6693–6705
33. Magrioti V, Nikolaou A, Smyrniotou A, et al. New potent and selective polyfluoroalkyl ketone inhibitors of GVIA calcium-independent phospholipase A$_2$. Bioorg Med Chem 2013;21:5823–5829
34. Ramanadham S, Bohrer A, Mueller M, Jett P, Gross RW, Turk J. Mass spectrometric identification and quantitation of arachidonate-containing phospholipids in pancreatic islets: prominence of plasmenylethanolamine molecular species. Biochemistry 1993;32:5339–5351
35. Ramanadham S, Gross RW, Han X, Turk J. Inhibition of arachidonate release by secretagogue-stimulated pancreatic islets suppresses both insulin secretion and the rise in beta-cell cytosolic calcium ion concentration. Biochemistry 1993;32:337–346
36. Carrero JA, Calderon B, Towfic F, Artyomov MN, Unanue ER. Defining the transcriptional and cellular landscape of type 1 diabetes in the NOD mouse. PLoS One 2013;8:e59701
37. Mandrup-Poulsen T, Nerup J, Reimers JI, et al. Cytokines and the endocrine system. II. Roles in substrate metabolism, modulation of thyroidal and pancreatic endocrine cell functions and autoimmune endocrine diseases. Eur J Endocrinol 1996;134:21–30
38. Ming WJ, Bersani L, Mantovani A. Tumor necrosis factor is chemotactic for monocytes and polymorphonuclear leukocytes. J Immunol 1987;138:1469–1474
39. Gil-de-Gómez L, Astudillo AM, Guijas C, et al. Cytosolic group IVA and calcium-independent group VIA phospholipase A$_2$s act on distinct phospholipid pools in zymosan-stimulated mouse peritoneal macrophages. J Immunol 2014;192:752–762
40. Bao S, Li Y, Lei X, et al. Attenuated free cholesterol loading-induced apoptosis but preserved phospholipid composition of peritoneal macrophages from mice that do not express group VIA phospholipase A$_2$. J Biol Chem 2007;282:27100–27114
41. Hinman RM, Smith MJ, Cambier JC. B cells and type 1 diabetes ...in mice and men. Immunol Lett 2014;160:128–132
42. Wong FS, Wen L, Tang M, et al. Investigation of the role of B-cells in type 1 diabetes in the NOD mouse. Diabetes 2004;53:2581–2587
43. Ganapathy V, Gurlo T, Jarstadmarken HO, von Grafenstein H. Regulation of TCR-induced IFN-gamma release from islet-reactive non-obese diabetic CD8($^+$) T cells by prostaglandin E(2) receptor signaling. Int Immunol 2000;12:851–860
44. Green-Mitchell SM, Tersey SA, Cole BK, et al. Deletion of 12/15-lipoxygenase alters macrophage and islet function in NOD-Alox15(null) mice, leading to protection against type 1 diabetes development. PLoS One 2013;8:e56763
45. Bao S, Song H, Wohltmann M, et al. Insulin secretory responses and phospholipid composition of pancreatic islets from mice that do not express Group VIA phospholipase A$_2$ and effects of metabolic stress on glucose homeostasis. J Biol Chem 2006;281:20958–20973
46. Ramanadham S, Hsu FF, Bohrer A, Ma Z, Turk J. Studies of the role of group VI phospholipase A$_2$ in fatty acid incorporation, phospholipid remodeling, lysophosphatidylcholine generation, and secretagogue-induced arachidonic acid release in pancreatic islets and insulinoma cells. J Biol Chem 1999;274:13915–13927
47. Bao S, Jacobson DA, Wohltmann M, et al. Glucose homeostasis, insulin secretion, and islet phospholipids in mice that overexpress iPLA$_2$β in pancreatic β-cells and in iPLA$_2$β-null mice. Am J Physiol Endocrinol Metab 2008;294:E217–E229
48. Lei X, Zhang S, Bohrer A, Ramanadham S. Calcium-independent phospholipase A$_2$ (iPLA$_2$ β)-mediated ceramide generation plays a key role in the cross-talk between the endoplasmic reticulum (ER) and mitochondria during ER stress-induced insulin-secreting cell apoptosis. J Biol Chem 2008;283:34819–34832